Communications in Computational Chemistry
Commun. Comput. Chem., Vol. 1, No. 2, 127–133
doi: 10.4208/cicc.2025.98.01
Regular Article

Molecular Insight into Energy Loss in Organic Solar Cells

Guangchao Han[1,*] and Yuanping Yi[1,2,*]

[1]*Beijing National Laboratory for Molecular Sciences, CAS Key Laboratory of Organic Solids, Institute of Chemistry, Chinese Academy of Sciences, Beijing 100190, China;*

[2]*University of Chinese Academy Sciences, Beijing 100049, China.*

[*] Corresponding author: gchaohan@iccas.ac.cn

Received on 08 April 2025; Accepted on 10 May 2025

Abstract: With the rapid development of A-D-A non-fullerene acceptors, organic solar cells (OSCs) have made significant progress. However, compared to inorganic and perovskite solar cells, the energy loss in OSCs remains relatively large. In this Perspective, we summarize our recent computational advances in elucidating the mechanisms of energy loss in OSCs at the molecular level. We highlight strategies to minimize voltage loss during charge generation, suppress triplet-channel recombination, and reduce non-radiative voltage loss by modulating both molecular and aggregation structures.

Key words: organic solar cells, voltage loss, triplet recombination, aggregation, multiscale simulations.

Introduction

Organic solar cells (OSCs) hold great promise for applications in building-integrated photovoltaics and wearable electronics, due to their unique advantages of light weight, flexibility, semi-transparency, and suitability for large-area solution processing.[1] The active layer of OSCs typically consists of electron-donor and electron-acceptor semiconducting materials, which are blended to form nanoscale phase-separated morphologies. Because of the low dielectric constants of organic semiconductors, absorption of sunlight forms Frenkel excitons. To produce photocurrent, these excitons need to diffuse to the donor/acceptor (D/A) interface and split into free charge carriers (FC). Subsequently, the free holes and electrons migrate along the donor and acceptor materials toward and are collected by the anode and cathode, respectively. Meanwhile, charge recombination, which occurs during generation and migration, should be suppressed. From the perspective of excited states, dissociation of the photogenerated singlet excitons (S_1) into FC is mediated by singlet charge-transfer (CT) states, while non-geminate recombination of FC leads to the formation of both singlet and triplet CT excitons ($^{S}CT_1$ and $^{T}CT_1$) in 1:3 ratio following the spin statistics (**Figure 1**) [2,3]. The $^{S}CT_1$ states can decay into the ground state (S_0) via radiative and non-radiative pathways. The recombination of the $^{T}CT_1$ states occurs through the low-lying triplet excitons (T_1, usually on the narrow-bandgap materials), which constitutes a major terminal loss channel of photocurrent.

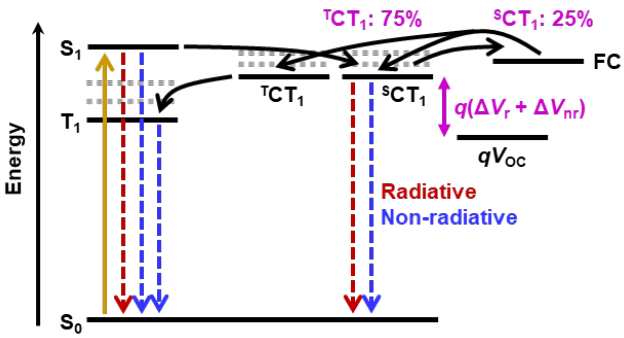

Figure 1. Excited-state Jablonski diagram for describing the charge generation and energy loss processes in organic solar cells.

The open-circuit voltage (V_{OC}) in OSCs is determined by the energy of the lowest CT states (E_{CT}), as well as recombination processes [4]. The requirement for exciton dissociation (ED) driving forces (ΔE_{CT}, i.e., the energy difference between S_1 and $^{S}CT_1$ states) thus leads to an extra voltage loss. According to the detailed balance theory (first

proposed by Shockley and Queisser), the voltage loss due to radiative recombination (ΔV_r) is inevitable (0.25-0.3 V) for any type of solar cells, while the voltage loss due to non-radiative recombination (ΔV_{nr}) is intrinsically linked to the device's electroluminescence external quantum efficiency (EQE_{EL}):

$$\Delta V_{nr} = (-k_B T/q) * ln(EQE_{EL})$$

where k_B is the Boltzmann constant, T is temperature, and q is the elementary charge [5,6]. An ideal EQE_{EL} = 1 results in ΔV_{nr} = 0, whereas a reduction in EQE_{EL} by one order of magnitude increases the ΔV_{nr} by 0.058 V at room temperature. The EQE_{EL} can be expressed as:

$$EQE_{EL} = \gamma \Phi_{PL} \chi \eta_{out}$$

where γ is the charge balance factor (often engineered to be 1), Φ_{PL} is the photoluminescence quantum yield, χ is the fraction of recombination events that decay radiatively, and η_{out} is the photon out-coupling efficiency (typically about 0.3). For OSCs, Φ_{PL} is related to the rates of radiative (k_r) and non-radiative (k_{nr}) recombination of the ^{S}CT$_1$ state ($\Phi_{PL} = k_r/(k_r + k_{nr})$, with k_{nr} >> k_r in most cases), and the decay of T_1 to S_0 limits χ to below 25%. Therefore, to simultaneously reduce both photocurrent and voltage losses, it is essential to suppress non-radiative recombination of the ^{S}CT$_1$ state and the triplet recombination channel.

In the early stage of OSC development, fullerene derivatives (e.g., PC$_{71}$BM), renowned for their excellent electron-accepting and electron-transporting properties, were the primary choice for acceptor materials [7]. Due to the weak visible and near-infrared absorption of fullerenes, fullerene-based OSCs commonly use narrow- or medium-bandgap small molecules or polymers as donors (e.g., PffBT4T-2OD, also known as PCE11) [8]. However, fullerene-based OSCs require a large ED driving force (ΔE_{CT} >0.3 eV) and suffer from severe non-radiative voltage losses (ΔV_{nr} >0.3 V), limiting their power conversion efficiencies (PCEs) to 11-12%. The emergence of narrow-bandgap A-D-A-type small-molecule acceptors (e.g., IT-4F and Y6) has changed the landscape [9,10]. Non-fullerene OSCs can achieve high-yield charge generation with a near-zero ΔE_{CT} and have a smaller ΔV_{nr} of ~0.2 V [11,12]. When combined with Y6 derivatives and wide-bandgap D-A copolymer donors (PM6 and D18), the highest PCEs of non-fullerene OSCs have surpassed the 20% milestone [13-16]. Nevertheless, compared with those of inorganic and perovskite counterparts, the ΔV_{nr} of the state-of-the-art OSCs is still larger (e.g., only 0.027 V in high-quality GaAs devices) [17]. Moreover, the highest short-circuit current density (J_{SC}) and fill factor of OSCs just reach 85-90% of the Shockley-Queisser limit. Hence, to further enhance the organic photovoltaic performance, it is imperative to deeply understand the molecular origins of energy loss and develop effective strategies to mitigate it.

Multiscale theoretical simulations, which combine quantum chemistry (QC) calculations and molecular dynamics (MD) simulations, can provide insights into the mechanisms of charge generation, charge transport, and energy loss in OSCs at the molecular level [12,18-20]. In this Perspective, we focus on reviewing our recent computational efforts on energy loss, highlighting how to minimize voltage loss during charge generation, suppress the triplet recombination channel, and decrease non-radiative voltage loss. Prior to that, a computational protocol will be briefly introduced.

Computational protocol

The electronic structure and dynamics of excited states in OSCs rely on not only molecular structures but also aggregation structures. We adopt QC calculations to construct model intermolecular geometries and MD simulations to produce mesoscopic molecular packing morphology.[18] Note that, the solvent evaporation and thermal annealing processes can be reliably imitated by quasi-equilibrium MD. Then, excited-state electronic structure properties and intermolecular electronic couplings can be obtained by QC calculations. The electronic structure calculations are mainly conducted by (time-dependent) density functional theory, with tuned long-range corrected hybrid functionals to achieve reasonable accuracy.

Minimizing voltage loss during charge generation

To maximize V_{OC} and J_{SC} concurrently, the ΔE_{CT} must be minimized without sacrificing charge generation efficiency. In OSCs with low driving forces, exciton dissociation proceeds mostly through the ^{S}CT$_1$ state. This requires the electronic coupling between S_1 and ^{S}CT$_1$ (V_{ED}) to be strong enough. Meanwhile, the non-radiative decay from ^{S}CT$_1$ to S_0 should be suppressed. The k_{nr} of the ^{S}CT$_1$ state can be estimated using the Marcus-Levich-Jortner tunneling formalism:

$$k_{nr} = {V_{CR}}^2 \sqrt{\frac{\pi}{\hbar^2 \lambda_l k_B T}} \times \sum_{v=0}^{\infty} \left\{ exp(-S_{eff}) \frac{S_{eff}^v}{v!} exp\left[-\frac{(-E_{CT} + \lambda_l + v\hbar\omega_{eff})^2}{4\lambda_l k_B T} \right] \right\}$$

where V_{CR} denotes the electronic coupling between ^{S}CT$_1$ and S_0, $\hbar$ is the reduced Planck constant, λ_l is the low-frequency reorganization energy (including both intramolecular and external contributions), ω_{eff} is the effective frequency corresponding to the intramolecular high-frequency vibration modes, and S_{eff} is the Huang-Rhys factor associated with the effective mode [21]. To reduce k_{nr}, it is necessary to increase E_{CT} and/or decrease the corresponding electronic coupling and reorganization energy. As the first-order approximation, the E_{CT} can be expressed as $E_{CT} = \left(\left|E_{HOMO,D}\right| - \left|(E_{LUMO,A}\right|\right) + E_{Coul}$, where $|E_{HOMO,D}|$ is the energy of the highest occupied molecular orbital (HOMO) of the donor (or more strictly, the ionization potential of the donor), $|E_{LUMO,A}|$ is the energy of the lowest unoccupied molecular orbital (LUMO) of the acceptor (or the electron affinity of the acceptor), and E_{Coul} represents the interfacial electron-hole Coulomb interaction energy. It is well-established that V_{ED}, V_{CR}, and E_{Coul} are all highly dependent on the D/A intermolecular relative orientations/positions [2,22].

To this end, we employed MD simulations to uncover the interfacial geometries in non-fullerene OSCs [23,24]. For example, in a representative all-small-molecule OSC of DRTB-T:IT-4F, IT-4F was found to be docked with the donor DRTB-T (also of the A-D-A-type) mainly via local π-π interaction between their electron-withdrawing end-groups (**Figure 2**a,b) [23]. This is due to the large steric hindrance of side chains on the backbone core, especially for IT-4F. Further QC calculations demonstrate that as IT-4F moves from the core to the terminal units of DRTB-T, both E_{Coul} (from approximately -0.3 to -0.2 eV) and V_{CR} (from around 22 to 8 meV) weaken significantly (Figure 2c). This is beneficial for suppressing ^{S}CT$_1$ decay and facilitating charge separation (CS). Although V_{ED} also decreases because the HOMO of DRTB-T is more concentrated on the electron-donating units, it remains sufficiently large (~5 meV)

to ensure efficient ED under low driving forces [with estimated rates of 10^{11}-10^{12} s^{-1}, which are much faster than the S_1 decay rate of IT-4F (~2.8×10^9 s^{-1})[25]]. Importantly, this favorable interfacial arrangement is the most probable in the blend. For non-fullerene OSCs based on D-A copolymer donors, the A-D-A acceptor and the polymer donor also prefer to interact with each other through their electron-withdrawing units [24]. Unlike A-D-A donors, the HOMO of polymer donors tends to delocalize over the entire backbone, leading to V_{ED} and V_{CR} both being larger, particularly for V_{CR}. Notably, such HOMO delocalization can reduce the reorganization energy from the cationic state to S_0 (e.g., only 0.078 eV for D18) [26]. Given that the reorganization energy from the anionic state to S_0 for A-D-A acceptors with rigid and extended central units is also quite small (e.g., 0.077 eV for Y6), the reorganization energy between $^SCT_1$ and S_0 is considerably lower than the $^SCT_1$ energy. Thus, the $^SCT_1$ decay is in the Marcus inverted region and can be effectively prevented. Indeed, the k_{nr} of the $^SCT_1$ state is much slower than the rate of the first CS step (by about two orders of magnitude) [27].

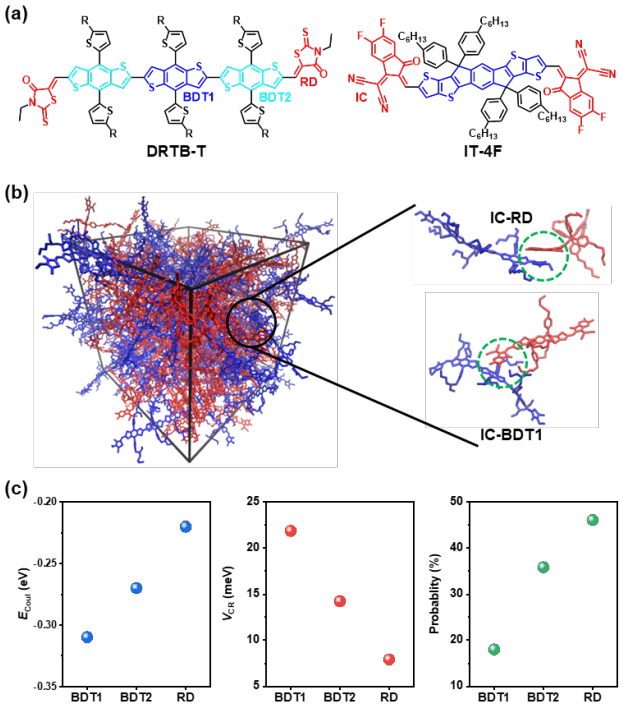

Figure 2. (a) Chemical structures of DRTB-T (R = 2-ethylhexyl) and IT-4F. (b) Two representative interfacial geometries (IC-RD and IC-BDT1) extracted from the MD-simulated DRTB-T:IT-4F blending film. (c) Average electronic coupling from $^SCT_1$ to S_0 (V_{CR}), average electron-hole Coulomb interaction energy (E_{Coul}), and probability of docking IT-4F with each unit of DRTB-T. Adapted with permission from ref 23. Copyright 2018 Wiley-VCH.

Compared to their small-molecule counterparts, polymerized small-molecule acceptors, achieved through end-group polymerization, exhibit superior thermal and light stability [28]. This makes them promising candidates for practical applications. In all-polymer OSCs, efficient CS requires fast intrachain charge transfer. Our QC calculations show that the intrachain electron transfer in these polymerized acceptors is dominated by π-bridge mediated super-exchange coupling [20,29]. Importantly, this coupling can be greatly enhanced by fine-tuning the linking positions, end-groups, and π-bridges.

During CS from the D/A interface, the proportions of donor and acceptor components surrounding holes and electrons gradually change. As a result, the polarization energies for donor holes (P_D^+) and acceptor electrons (P_A^-) are varied, leading to energy level bending near the interface. As illustrated in **Figure 3**a, if P_D^+ and P_A^- are increased from the interface to the pure bulk (ΔP >0), the Coulomb attraction in the CT states will be compensated, thereby reducing the CS energy barrier (ΔE_{CS}). To clarify the role of electronic polarization in CS, we mimicked a series of D/A heterojunctions (including DRTB-T/$PC_{71}BM$, DRTB-T:IT-4F, and BTR-Cl/Y6) using atomistic MD simulations and calculated the P_D^+ and P_A^- values via a polarizable force field method (Figure 3b,c) [30]. In the case of DRTB-T/$PC_{71}BM$, both P_D^+ and P_A^- decrease (ΔP < 0), resulting in an increase in ΔE_{CS}. Therefore, in fullerene-based OSCs, a large ΔE_{CT} is generally required to afford an excess energy for facilitating CS through high-lying CT states. By contrast, for non-fullerene OSCs based on A-D-A acceptors, the polarization energies, especially P_A^-, are enhanced (ΔP > 0). This is primarily ascribed to the strong stabilization of electrons but destabilization of holes by electrostatic interactions in the A-D-A acceptors. Remarkably, in the IT-4F and Y6 based heterojunctions, the ΔP can completely overcome the Coulomb attraction, leading to barrier-free CS (e.g., a negative ΔE_{CS} of -0.24 eV for BTR-Cl:Y6).

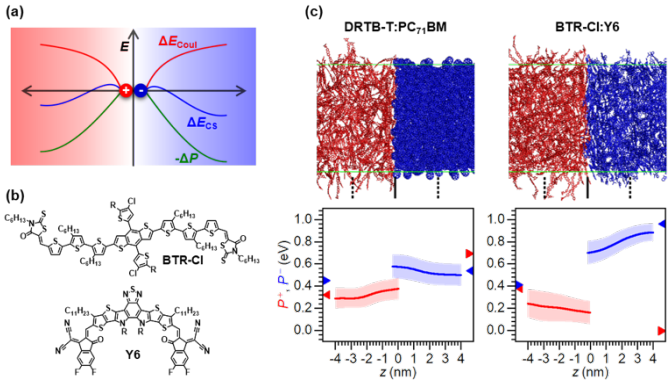

Figure 3. (a) Schematic description of polarization assisted CS. (b) Chemical structures of BTR-Cl and Y6 (R = 2-ethylhexyl). (c) P_D^+ and P_A^- as a function of the distance of the charge carriers from the interface for MD simulated DRTB-T:$PC_{71}BM$ and BTR-Cl:Y6 heterojunctions. Adapted with permission from ref 28. Copyright 2020 American Chemical Society.

Suppressing triplet-channel recombination

From an energetic point of view, suppressing the triplet recombination channel requires the T_1 energy to be close to or higher than that of the $^TCT_1$ state. Therefore, it is crucial to reduce the S_1-T_1 energy gap (ΔE_{ST}), particularly for OSCs with low driving forces [31]. Although maximizing the intramolecular push-pull effect (i.e., minimizing the overlap between the HOMO and LUMO wave functions) can dramatically decrease ΔE_{ST}, it inevitably leads to reduced oscillator strength (*f*) and weak light absorption for the S_1 state. It is important to note that the intermolecular couplings for singlet and triplet excitons are governed by long-range Coulombic and short-range exchange interactions, respectively. This means that ΔE_{ST} can be modulated by molecular aggregates [32]. As illustrated in **Figure 4**a, for V- and J-type dimers, the triplet energy splitting is

negligible, while the singlet energy splitting remains significant and the lower-energy state or both splitting states are transition dipole-allowed. Consequently, the ΔE_{ST} can be substantially reduced. Moreover, the red-shifted or broadened absorption spectra are beneficial to improving J_{SC}. In contrast, H-aggregation gives rise to a blue-shift of the absorption spectra and an increase in ΔE_{ST}.

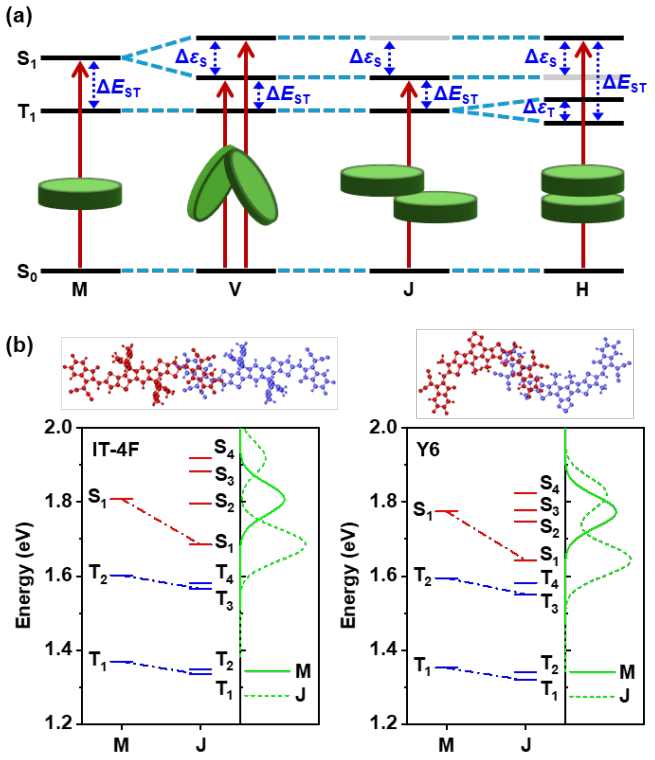

Figure 4. (a) Schematic diagram of the splitting energies for the S_1 and T_1 states ($\Delta\varepsilon_S$ and $\Delta\varepsilon_T$) and the ΔE_{ST} in the monomer (M) and the V-, J- and H-type dimers with different packing motifs. (b) Energy level alignment of the singlet and triplet excited states and absorption spectra for the monomer and J-type dimer of IT-4F and Y6. Adapted with permission from ref 30. Copyright 2020 Wiley-VCH.

Intriguingly, the π-π stacking between the electron-withdrawing terminal units, which frequently appears in the films or crystals of A-D-A acceptors, belongs to the J- or V-type dimers [14-16,20,32]. Owing to a modest intramolecular push-pull effect, these acceptors exhibit a moderate ΔE_{ST} of 0.4-0.5 eV while maintaining a large f (~3) in the monomers (Figure 4b). Importantly, QC calculations on model end-group π-π stacking dimers (or dimers extracted from MD-simulated films) demonstrate that ΔE_{ST} can be reduced to 0.3-0.4 eV due to the significant decrease in S_1 energy. Moreover, such small ΔE_{ST} has proved to be able to effectively inhibit the triplet-channel recombination when ΔE_{CT} is small (<0.2 eV); the estimated rates of T_1 back to $^TCT_1$ are much faster than the rates of T_1 decay via intersystem crossing (by over three orders of magnitude). This can contribute to a high fill factor (~80%) for low-driving-force OSCs based on A-D-A acceptors, even with only moderate charge mobilities (~10^{-4} cm^2 V^{-1} s^{-1}) [13-16].

Notably, there are often multiple triplet states on the donor and/or acceptor materials below the S_1 state. This implies that $^TCT_1$ can interact with more than one local triplet state, especially in low-driving-force OSCs. Take a high-performance ZR1:Y6 OSC as an example (**Figure 5**a,b). When ZR1 and Y6 contact with each other via favorable end-group π-π stacking, the $^TCT_1$ state can be hybridized with multiple molecular triplet states that are lying below $^TCT_1$ due to strong intermolecular electronic couplings [33]. Importantly, the hybridization can cause considerable energetic inversion between $^SCT_1$ and $^TCT_1$ and destabilize the $^TCT_1$ state at close donor:acceptor separations (Figure 5c). This enables the re-dissociation of the $^TCT_1$ state, thereby improving EQE_{EL} and reducing ΔV_{nr} [34]. However, when $^TCT_1$ lies among these local triplet states (appearing in the complexes with more intermolecular overlap), the destabilization of the $^TCT_1$ state induced by the hybridization with the under triplet states can be compensated by the hybridization with the upper triplet states. Therefore, to prevent T_1 formation, it is critical to precisely control the interfacial geometries to achieve the $^SCT_1/^TCT_1$ energetic inversion.

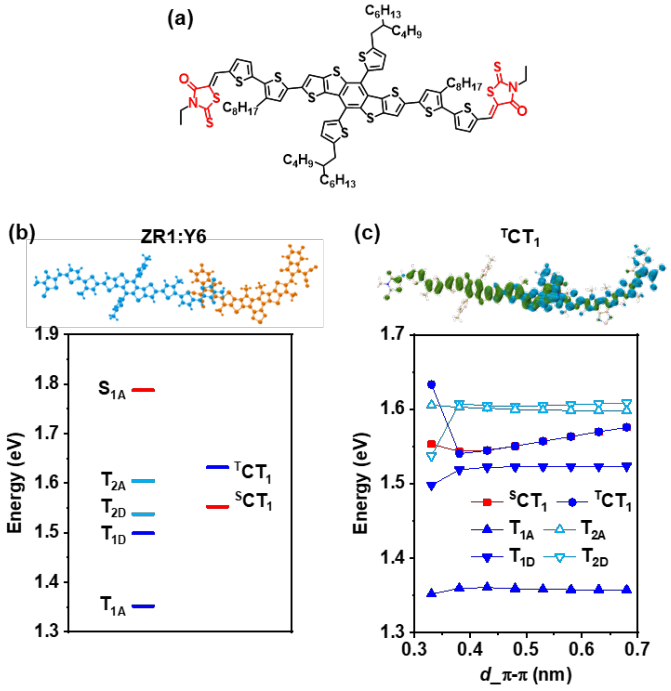

Figure 5. (a) Chemical structure of ZR1 (a high-performance A-D-A-type small-molecule donor). (b) Energy level alignment of the singlet and triplet excited states for a terminal π-π stacking complex of ZR1:Y6. (c) Electron-hole density map of $^TCT_1$ (blue: electron; green: hole) and rigid scan of the excited-state energies as a function of the intermolecular separation (d_π-π) for the ZR1:Y6 complex. Adapted with permission from ref 31. Copyright 2024 Royal Society of Chemistry.

Reducing non-radiative voltage loss

The radiative decay rate of the $^SCT_1$ state ($k_r \propto E_{CT}{}^2 f$, according to the Einstein coefficient relation) in fullerene-based OSCs is generally very slow, due to the quite small f of the $^SCT_1$ state. Thus, the Φ_{PL} and EQE_{EL} are rather low and primarily determined by the non-radiative decay rate of the $^SCT_1$ state. Indeed, the ΔV_{nr} in these OSCs is large and increases dramatically as E_{CT} decreases [35]. Recent advances in non-fullerene OSCs come with reduced ΔV_{nr} and the ΔV_{nr} values show no energy-gap law dependence [11]. This can be well explained by our excited-state calculations for the model

DRTB-T:IT-4F complexes [27]. As displayed in **Figure 6**a, the $^{S}CT_1$ state can borrow considerable oscillator strength from the energy-close S_1 state on the narrow-bandgap A-D-A acceptor (S_{1A}). Furthermore, upon acceptor J-aggregation, the S_{1A} state is even fully hybridized with the $^{S}CT_1$ state. The enhanced oscillator strength of the $^{S}CT_1$ or $^{S}CT_1/S_{1A}$ state can significantly improve Φ_{PL} and reduce ΔV_{nr}. Therefore, it is indispensable to involve the highly emissive S_1 state for obtaining a reliable description of the dynamics of the $^{S}CT_1$ state in low-driving-force OSCs. This also implies that the luminescence efficiency of the pristine narrow-bandgap material defines the lower limit of ΔV_{nr}. To improve the Φ_{PL}, it is imperative to avoid the formation of H-aggregation and promote the formation of J-aggregation (Figure 4a). Moreover, it should be noted that the state-of-the-art Y6-type acceptors can form tightly packed aggregates, leading to the formation of low-lying excited states with strong intermolecular CT character (Figure 6b) [36]. This suggests that moderately reducing the intermolecular interaction of Y6-type acceptors is conducive to improving the Φ_{PL} while maintaining efficient charge transport.

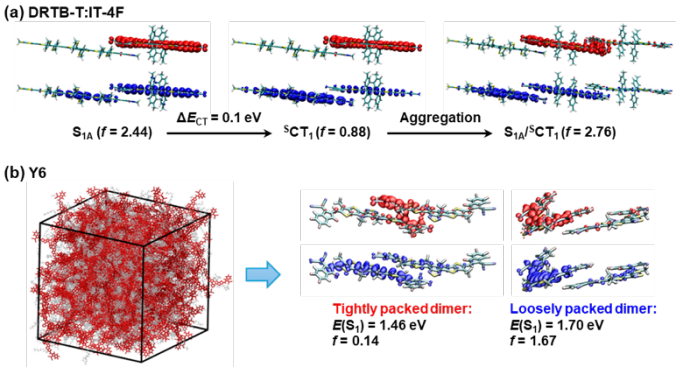

Figure 6. Electron-hole density maps (red: electron; blue: hole) and oscillator strengths (*f*) for the lowest singlet excited states of (a) the DRTB-T:IT-4F complexes (built via end-group π-π stacking) and (b) the Y6 dimers (extracted from MD-simulated film). (a) Adapted with permission from ref 27. Copyright 2019 American Chemical Society. (b) Adapted with permission from ref 34. Copyright 2024 Royal Society of Chemistry.

It should be noted that molecular vibrations and the diversity of molecular conformations inevitably contribute to broad distributions in the transport energy levels of OSCs [37]. This energetic disorder (here, labelled as σ_H and σ_L for the E_{HOMO} and E_{LUMO} distributions, respectively) not only reduces charge mobility but also results in significant $^{S}CT_1$-state energetic disorder (σ_{CT}). Within the broadened E_{CT} distribution, the occupation of low-lying CT states will accelerate non-radiative recombination, as dictated by the energy-gap law. Thus, reducing σ_{CT} can directly increase V_{OC} while diminishing ΔV_{nr}. To explore the source of σ_{CT}, we systematically investigated the energetic disorder in representative polymer OSCs (including PCE11:$PC_{71}BM$ and PM6:Y6) by means of multiscale theoretical simulations (**Figure 7**) [38]. The results indicate that, regardless of whether the OSCs are based on fullerene or A-D-A acceptors, the σ_H of polymer donors (PCE11: 116 meV; PM6: 68 meV) is significantly larger than the σ_L of acceptors ($PC_{71}BM$: 56 meV; Y6: 51 meV). Moreover, the σ_H of polymer donors matched with fullerene acceptors (e.g., PCE11) is much greater than that of polymer donors matched with A-D-A acceptors (e.g., PM6). This implies that, counter-intuitively, the decrease in σ_{CT} from fullerene-based to A-D-A acceptor-based OSCs is mainly attributed to changes in the polymer donors rather than the acceptors. Importantly, we identified two key design principles for reducing the σ_H of polymer donors. The first is the adoption of small fused-ring units, which can not only decrease the conformational degree of freedom but also allow side chains to be far from the main-chain torsion angles (e.g., from PCE11 to PM6). The second is the introduction of conformational locks into the electron-donating moieties where the HOMO shows more distribution. Besides, narrowing the distribution of E_{Coul} by reducing the diversity of interfacial arrangements (e.g., via side-chain engineering) is also needed for further lowering σ_{CT}.

Summary and outlook

To gain insights into the microscopic mechanisms governing energy loss in OSCs, we have employed advanced theory and simulations to accurately characterize the electronic structure properties of excited states in archetypal organic photovoltaic systems. The key findings are summarized as follows:

(1) For non-fullerene OSCs, enhancing contact between the electron-withdrawing units of donor and acceptor molecules helps suppress non-radiative recombination of the $^{S}CT_1$ state while keeping efficient ED. Importantly, the polarization energies of holes and electrons are enhanced during CS, which can compensate for the Coulomb attraction in the CT states and even lead to barrierless CS in the systems based on fluorinated A-D-A acceptors. This suggests that the energy loss during charge generation can be minimized.

(2) Reducing ΔE_{ST}, particularly in narrow-bandgap materials, is critical for suppressing the triplet recombination channel. Notably, the ΔE_{ST} of A-D-A acceptors can be effectively reduced through end-group π-π stacking while maintaining strong light absorption. Interestingly, the $^{T}CT_1$ state can hybridize with multiple molecular triplet states. When $^{T}CT_1$ is near the upper edge of the local triplet manifold, this hybridization can destabilize the $^{T}CT_1$ state, which is beneficial for preventing T_1 formation. This mechanism offers another feasible route to decrease the triplet-channel energy loss under low driving forces.

(3) In non-fullerene OSCs, low driving forces can induce hybridization of the $^{S}CT_1$ state with the highly emissive S_1 state on the A-D-A acceptors, enhancing luminescence efficiency and reducing non-radiative voltage loss. From fullerene-based to A-D-A acceptor-based polymer OSCs, the reduction of interfacial energetic disorder is primarily owing to variations in the polymer donors rather than the acceptors. This indicates that optimizing polymer donors is key for further reducing non-radiative voltage loss.

Overall, these computational studies provide a molecular understanding of energy loss in OSCs, paving the way for improved photovoltaic performance through the fine-tuning of both molecular and aggregation structures. However, multiscale theoretical simulations are computationally intensive. Data-driven machine learning offers a promising approach to expediate the identification of potential D/A pairs with low energy loss [31].

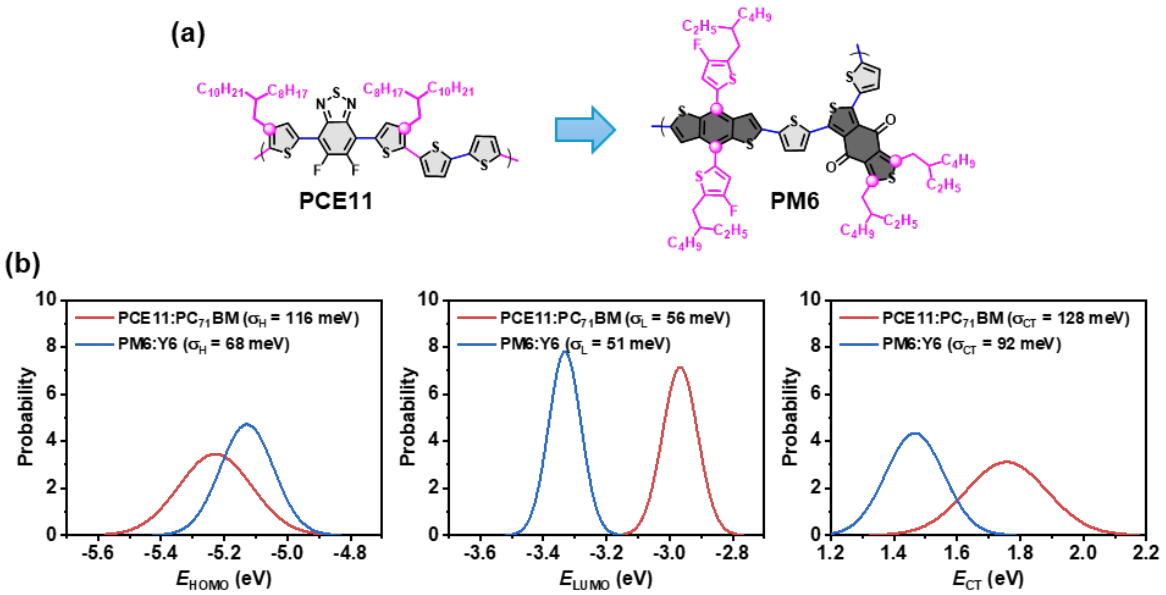

Figure 7. (a) Chemical structures of PCE11 and PM6. (b) Distributions of E_{HOMO}, E_{LUMO}, and E_{CT} as well as their corresponding degrees of disorder (σ_H, σ_L, and σ_{CT}) in the PCE11:PC_{71}BM and PM6:Y6 blends. Adapted with permission from ref 36. Copyright 2025 American Chemical Society.

Acknowledgements

This work is supported by the Youth Innovation Promotion Association CAS (Grant 2023037).

References

[1] Hu Y., Wang J., Yan C., Cheng P. The multifaceted potential applications of organic photovoltaics. *Nat. Rev. Mater.*, **7** (11) (2022), 836-838.

[2] Brédas J.-L., Norton J.E., Cornil J., Coropceanu V. Molecular understanding of organic solar cells: the challenges. *Acc. Chem. Res.*, **42** (11) (2009), 1691-1699.

[3] Rao A., Chow P.C.Y., Gélinas S., Schlenker C.W., Li C.-Z., Yip H.-L., Jen A.K.Y., Ginger D.S., Friend R.H. The role of spin in the kinetic control of recombination in organic photovoltaics. *Nature*, **500** (2013), 435.

[4] Vandewal K., Tvingstedt K., Gadisa A., Inganäs O., Manca J.V. On the origin of the open-circuit voltage of polymer–fullerene solar cells. *Nat. Mater.*, **8** (2009), 904.

[5] Shockley W., Queisser H.J. Detailed balance limit of efficiency of p-n junction solar cells. *J. Appl. Phys.*, **32** (3) (1961), 510-519.

[6] Rau U. Reciprocity relation between photovoltaic quantum efficiency and electroluminescent emission of solar cells. *Phys. Rev. B*, **76** (8) (2007), 085303.

[7] He Y., Li Y. Fullerene derivative acceptors for high performance polymer solar cells. *Phys. Chem. Chem. Phys.*, **13** (6) (2011), 1970-1983.

[8] Liu Y., Zhao J., Li Z., Mu C., Ma W., Hu H., Jiang K., Lin H., Ade H., Yan H. Aggregation and morphology control enables multiple cases of high-efficiency polymer solar cells. *Nat. Commun.*, **5** (2014), 5293.

[9] Zhao W., Li S., Yao H., Zhang S., Zhang Y., Yang B., Hou J. Molecular optimization enables over 13 % efficiency in organic solar cells. *J. Am. Chem. Soc.*, **139** (21) (2017), 7148-7151.

[10] Yuan J., Zhang Y., Zhou L., Zhang G., Yip H.-L., Lau T.-K., Lu X., Zhu C., Peng H., Johnson P.A., Leclerc M., Cao Y., Ulanski J., Li Y., Zou Y. Single-junction organic solar cell with over 15 % efficiency using fused-ring acceptor with electron-deficient core. *Joule*, **3** (4) (2019), 1140-1151.

[11] Chen X.-K., Qian D., Wang Y., Kirchartz T., Tress W., Yao H., Yuan J., Hülsbeck M., Zhang M., Zou Y., Sun Y., Li Y., Hou J., Inganäs O., Coropceanu V., Brédas J.-L., Gao F. A unified description of non-radiative voltage losses in organic solar cells. *Nat. Energy*, **6** (2021), 799-806.

[12] Han G., Yi Y. Molecular insight into efficient charge generation in low-driving-force nonfullerene organic solar cells. *Acc. Chem. Res.*, **55** (6) (2022), 869-877.

[13] Zhu L., Zhang M., Zhou G., Wang Z., Zhong W., Zhuang J., Zhou Z., Gao X., Kan L., Hao B., Han F., Zeng R., Xue X., Xu S., Jing H., Xiao B., Zhu H., Zhang Y., Liu F. Achieving 20.8 % organic solar cells via additive-assisted layer-by-layer fabrication with bulk p-i-n structure and improved optical management. *Joule*, **8** (11) (2024), 3153-3168.

[14] Jiang Y., Sun S., Xu R., Liu F., Miao X., Ran G., Liu K., Yi Y., Zhang W., Zhu X. Non-fullerene acceptor with asymmetric structure and phenyl-substituted alkyl side chain for 20.2 % efficiency organic solar cells. *Nat. Energy*, **9** (2024), 975-986.

[15] Chen H., Huang Y., Zhang R., Mou H., Ding J., Zhou J., Wang Z., Li H., Chen W., Zhu J., Cheng Q., Gu H., Wu X., Zhang T., Wang Y., Zhu H., Xie Z., Gao F., Li Y., Li Y. Organic solar cells with 20.82 % efficiency and high tolerance of active layer thickness through crystallization sequence manipulation. *Nat. Mater.*, **24** (2025), 444-453.

[16] Li C., Song J., Lai H., Zhang H., Zhou R., Xu J., Huang H., Liu L., Gao J., Li Y., Jee M.H., Zheng Z., Liu S., Yan J., Chen X.-K., Tang Z., Zhang C., Woo H.Y., He F., Gao F., Yan H., Sun Y. Non-fullerene acceptors with high crystallinity and photoluminescence quantum yield enable > 20 % efficiency organic solar cells. *Nat. Mater.*, **24** (2025), 433-443.

[17] Liu Q., Vandewal K. Understanding and suppressing non-radiative recombination losses in non-fullerene organic solar cells. *Adv. Mater.*, **35** (35) (2023), 2302452.

[18] Han G., Yi Y. From molecular packing structures to electronic processes: theoretical simulations for organic solar cells. *Adv. Energy Mater.*, **8** (2018), 1702743.

[19] Han G., Yi Y. Origin of photocurrent and voltage losses in organic solar cells. *Adv. Theory Simul.*, **2** (8) (2019), 1900067.

[20] Han G., Zhang Y., Zheng W., Yi Y. Electron transport in organic photovoltaic acceptor materials: improving the carrier mobilities by intramolecular and intermolecular modulations. *J. Phys. Chem. Lett.*, **14** (19) (2023), 4497-4503.

[21] Ridley J., Zerner M. An intermediate neglect of differential overlap technique for spectroscopy: pyrrole and the azines. *Theoret. Chim. Acta*, **32** (2) (1973), 111-134.

[22] Han G., Guo Y., Duan R., Shen X., Yi Y. Importance of side-chain anchoring atoms on electron donor/fullerene interfaces for high-performance organic solar cells. *J. Mater. Chem. A*, **5** (19) (2017), 9316-9321.

[23] Han G., Yi Y. Rationalizing small-molecule donor design toward high-performance organic solar cells: perspective from molecular architectures. *Adv. Theory Simul.*, **1** (11) (2018), 1800091.

[24] Han G., Guo Y., Ma X., Yi Y. Atomistic insight into donor/acceptor interfaces in high-efficiency nonfullerene organic solar cells. *Sol. RRL*, **2** (11) (2018), 1800190.

[25] Firdaus Y., Le Corre V.M., Karuthedath S., Liu W., Markina A., Huang W., Chattopadhyay S., Nahid M.M., Nugraha M.I., Lin Y., Seitkhan A., Basu A., Zhang W., McCulloch I., Ade H., Labram J., Laquai F., Andrienko D., Koster L.J.A., Anthopoulos T.D. Long-range exciton diffusion in molecular non-fullerene acceptors. *Nat. Commun.*, **11** (1) (2020), 5220.

[26] Cao Z., Yang S., Wang B., Shen X., Han G., Yi Y. Multi-channel exciton dissociation in D18/Y6 complexes for high-efficiency organic photovoltaics. *J. Mater. Chem. A*, **8** (39) (2020), 20408-20413.

[27] Han G., Yi Y. Local excitation/charge-transfer hybridization simultaneously promotes charge generation and reduces nonradiative voltage loss in nonfullerene organic solar cells. *J. Phys. Chem. Lett.*, **10** (11) (2019), 2911-2918.

[28] Zhang Z.-G., Li Y. Polymerized small-molecule acceptors for high-performance all-polymer solar cells. *Angew. Chem. Int. Ed.*, **60** (9) (2021), 4422-4433.

[29] Zhang Y., Han G., Yi Y. Electronic, optical, and charge transport properties of dimerized small-molecule acceptors: the role of end-group engineering. *Sci. China Mater.*, **68** (2024), 1480-1488.

[30] Tu Z., Han G., Yi Y. Barrier-free charge separation enabled by electronic polarization in high-efficiency non-fullerene organic solar cells. *J. Phys. Chem. Lett.*, **11** (7) (2020), 2585-2591.

[31] Han G., Yi Y. Singlet-triplet energy gap as a critical molecular descriptor for predicting organic photovoltaic efficiency. *Angew. Chem. Int. Ed.*, **61** (49) (2022), e202213953.

[32] Han G., Hu T., Yi Y. Reducing the singlet-triplet energy gap by end-group π-π stacking toward high-efficiency organic photovoltaics. *Adv. Mater.*, **32** (22) (2020), 2000975.

[33] Miao X., Han G., Yi Y. Energetic inversion of singlet/triplet interfacial charge-transfer states for reduced energy loss in organic solar cells. *J. Mater. Chem. A*, **12** (19) (2024), 11295-11301.

[34] Gillett A.J., Privitera A., Dilmurat R., Karki A., Qian D., Pershin A., Londi G., Myers W.K., Lee J., Yuan J., Ko S.-J., Riede M.K., Gao F., Bazan G.C., Rao A., Nguyen T.-Q., Beljonne D., Friend R.H. The role of charge recombination to triplet excitons in organic solar cells. *Nature*, **597** (7878) (2021), 666-671.

[35] Benduhn J., Tvingstedt K., Piersimoni F., Ullbrich S., Fan Y., Tropiano M., McGarry K.A., Zeika O., Riede M.K., Douglas C.J., Barlow S., Marder S.R., Neher D., Spoltore D., Vandewal K. Intrinsic non-radiative voltage losses in fullerene-based organic solar cells. *Nat. Energy*, **2** (2017), 17053.

[36] Guo Y., Han G., Guo J., Guo H., Fu Y., Miao X., Wang Z., Li D., Li S., Xu X., Lu X., Chen H., Yi Y., Chow P.C.Y. Engineering ultrafast exciton dynamics to boost organic photovoltaic performance. *Energy Environ. Sci.*, **17** (22) (2024), 8776-8786.

[37] Yuan J., Zhang C., Qiu B., Liu W., So S.K., Mainville M., Leclerc M., Shoaee S., Neher D., Zou Y. Effects of energetic disorder in bulk heterojunction organic solar cells. *Energy Environ. Sci.*, **7** (15) (2022), 2806-2818.

[38] Miao X., Han G., Yi Y. Toward low energetic disorder in organic solar cells: the critical role of polymer donors. *J. Phys. Chem. Lett.*, **16** (2025), 1987-1993.